Radiologic Assessment of Native Renal Vasculature: A Multimodality Review[1]

Sayf Al-Katib, MD
Monisha Shetty, MD
Syed Mohammad A. Jafri, MD
Syed Zafar H. Jafri, MD

Abbreviations: AVF = arteriovenous fistula, AVM = arteriovenous malformation, FMD = fibromuscular dysplasia, IVC = inferior vena cava, NF-1 = neurofibromatosis type 1, PSV = peak systolic velocity, RAA = renal artery aneurysm, RAS = renal artery stenosis

RadioGraphics 2017; 37:136–156

Published online 10.1148/rg.2017160060

Content Codes: CT GU MR US VA

[1]From the Department of Diagnostic Radiology and Molecular Imaging (S.A., M.S., S.Z.H.J.) and Department of Urology (S.M.A.J.), Beaumont Health, Oakland University William Beaumont School of Medicine, Royal Oak, 3601 W 13 Mile Rd, Royal Oak, MI 48073. Presented as an education exhibit at the 2015 RSNA Annual Meeting. Received March 13, 2016; revision requested May 19 and received June 11; accepted July 12. For this journal-based SA-CME activity, the authors, editor, and reviewers have disclosed no relevant relationships. **Address correspondence to** S.A. (e-mail: *Sayf.Al-katib@beaumont.org*).

SA-CME LEARNING OBJECTIVES

After completing this journal-based SA-CME activity, participants will be able to:

- Identify native renal vascular variants and describe their clinical implications.
- Describe the advantages and disadvantages of various imaging modalities in the detection of renal vascular disease and determine optimal imaging protocols.
- List the spectrum of pathologic conditions that can affect the native renal arteries and veins and the appropriate management of these entities.

See www.rsna.org/education/search/RG.

A wide range of clinically important anatomic variants and pathologic conditions may affect the renal vasculature, and radiologists have a pivotal role in the diagnosis and management of these processes. Because many of these entities may not be suspected clinically, renal artery and vein assessment is an essential application of all imaging modalities. An understanding of the normal vascular anatomy is essential for recognizing clinically important anatomic variants. An understanding of the protocols used to optimize imaging modalities also is necessary. Renal artery stenosis is the most common cause of secondary hypertension and is diagnosed by using both direct ultrasonographic (US) findings at the site of stenosis and indirect US findings distal to the stenosis. Fibromuscular dysplasia, while not as common as atherosclerosis, remains an important cause of renal artery hypertension, especially among young female individuals. Fibromuscular dysplasia also predisposes individuals to renal artery aneurysms and dissection. Although most renal artery dissections are extensions of aortic dissections, on rare occasion they occur in isolation. Renal artery aneurysms often are not suspected clinically before imaging, but they can lead to catastrophic outcomes if they are overlooked. Unlike true aneurysms, pseudoaneurysms are typically iatrogenic or posttraumatic. However, multiple small pseudoaneurysms may be seen with underlying vasculitis. Arteriovenous fistulas also are commonly iatrogenic, whereas arteriovenous malformations are developmental (ie, congenital). Both of these conditions involve a prominent feeding artery and draining vein; however, arteriovenous malformations contain a nidus of tangled vessels. Nutcracker syndrome should be suspected when there is distention of the left renal vein with abrupt narrowing as it passes posterior to the superior mesenteric artery. Filling defects in a renal vein can be due to a bland or tumor thrombus. A tumor thrombus is most commonly an extension of renal cell carcinoma. When an enhancing mass is located predominantly within a renal vein, leiomyosarcoma of the renal vein should be suspected.

Introduction

Vascular disease affecting the native renal arterial and venous system poses a unique challenge to radiologists. These challenges range from those faced in commonly encountered clinical scenarios, such as the workup of secondary hypertension or hematuria, to those related to rare and often clinically unsuspected diagnoses such as vasculitis. The radiologist's search protocol should include the renal vascular structures, as these are often clinically asymptomatic but may have important implications for disease management. When a vascular abnormality is suspected, imaging protocols can be tailored to optimize detection. In addition, it is important that the radiologist be able to recognize the vascular nature of lesions to avoid a catastrophic biopsy and appropriately direct disease management.

TEACHING POINTS

- US diagnostic criteria for RAS can be divided into direct signs, which are seen at the site of stenosis, and indirect signs, which are distal to the stenosis. Direct signs include a PSV greater than 200 cm/sec; a renal artery PSV–to–prerenal abdominal aorta PSV ratio higher than 3.5:1.0; the lack of a Doppler US signal, indicating occlusion; and the presence of color artifacts such as aliasing related to turbulence.
- In contradistinction to atherosclerotic stenoses, which are seen in the proximal renal artery, FMD-related stenoses tend to occur in the middle to distal portion of the renal artery.
- RAAs 1.0–1.5 cm in diameter should be evaluated with surveillance imaging every 1–2 years. Patients with RAAs larger than 1.5 cm should be referred for definitive treatment. Additional indications for treatment of RAAs include uncontrolled hypertension and symptomatic cases due to peripheral vascular bed embolism.
- It is especially important to recognize and consider the presence of crossing vessels owing to the associated risk for hemorrhage during minimally invasive therapies. Furthermore, the presence of crossing vessels decreases the success rate with antegrade endopyelotomy—reportedly from 86% to 42%. In addition, intraoperative preservation of crossing vessels is important for preserving renal function, as these vessels are end arteries, which lack an anastomotic communication.
- The diagnosis of renal vein leiomyosarcoma should be suspected when a mass with intravascular extension into the renal vein is present without an associated solid organ mass.

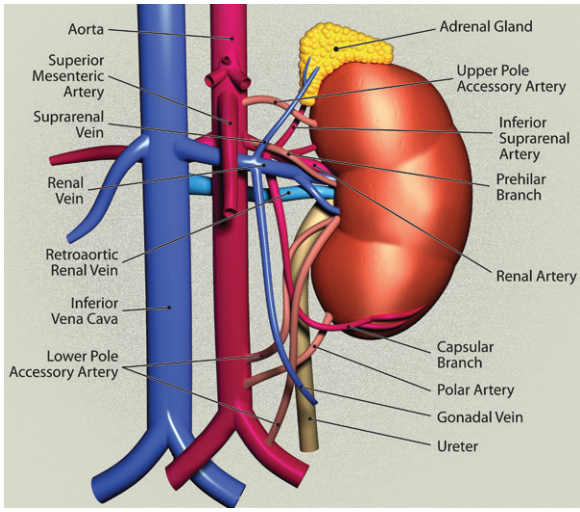

Figure 1. Drawing illustrates the normal and variant vascular anatomy of the kidney. The renal artery arises below the superior mesenteric artery and supplies arterial branches to the adrenal gland and capsular branches. Early branching vessels, also known as prehilar branches, arise less than 1.5–2.0 cm from the origin of the renal artery. Accessory renal arteries enter the renal hilum and may arise above or below the main renal artery. In contrast, polar arteries enter the kidney outside the hilum. The normal preaortic left renal vein passes posterior to the superior mesenteric artery and may receive tributaries from the lumbar, suprarenal, and gonadal veins. A retroaortic left renal vein may occur alone or as part of a circumaortic vein.

Anatomy

Approximately 20% of cardiac output is directed to the kidneys by way of the paired renal arteries (1). The main renal artery normally arises from the abdominal aorta, below the level of the superior mesenteric artery at the L2 vertebral body level (Fig 1) (2). The main renal artery is typically 4–6 cm in length and 5–6 mm in diameter. The right main renal artery is longer and often originates slightly superior to the left renal artery (1). The right renal artery is the only major vessel to course posterior to the inferior vena cava (IVC).

Accessory renal arteries are found in approximately 30% of individuals and are present bilaterally in 10% of individuals (1). Anomalous renal vasculature is much more common in patients who have renal fusion and positional anomalies. For example, more than 60% of patients with horseshoe kidney have multiple renal arteries arising from the aorta, iliac arteries, or even the inferior mesenteric artery (3). Likewise, there is wide variation in the renal vascular supply in patients with crossed fused renal ectopia (4). The fused kidneys may be supplied by a single renal artery or multiple renal arteries.

Accessory renal arteries can arise from the aorta or iliac arteries, anywhere from the T11 to L4 vertebral level. Rarely, an accessory renal artery may arise from the lower thoracic aorta. Accessory renal arteries more often arise below the main renal artery, and when they are present, they cross anterior to the ureter and have the potential to cause obstruction (1). In contrast to accessory renal arteries, which enter the kidney through the hilum, aberrant renal arteries, also known as polar arteries, enter the kidney through the capsule outside the hilum (5). Before kidney donation procedures, imaging is performed to assess the vasculature for multiple renal arteries, as the presence of more than two renal arteries is a relative contraindication to surgery (6).

The main renal artery supplies small branches to the adrenal gland, ureter, perinephric tissue, and renal capsule (1). Prehilar branches of the main renal artery that arise less than 1.5–2.0 cm from the origin should be noted in patients who are being evaluated as possible renal donors, because these early branches may complicate the surgical arterial anastomosis (6). Near the renal hilum, the main renal artery divides into segmental arteries that course through the renal sinus to supply five arterial segments of the kidney—specifically, the apical, superior, middle, inferior, and posterior segments (1). A relatively avascular plane known as the Brödel bloodless line of incision exists between the posterior segment and remaining anterior segments (2,7). This avascular plane is found at the junction of the anterior two-thirds

and posterior one-third of the kidney and considered an optimal route to minimize bleeding complications during percutaneous nephrostomy or anatrophic nephrolithotomy (7).

Vascular segments of the kidneys are supplied by end arteries, which lack an anastomotic communication. Segmental arteries branch into lobar arteries that supply an individual renal pyramid. Subsequent divisions of the lobar arteries include their branching into interlobar arteries and then into arcuate arteries; this area of branching indicates the true corticomedullary junction (Fig 2). Normally, resistance to blood flow increases progressively toward the more peripheral parenchymal vessels. Therefore, the pulsus parvus et tardus waveform that results from renal artery stenosis (RAS) will be most evident in the peripheral vasculature. The arcuate arteries divide into interlobular arteries that supply the afferent glomerular arterioles. The kidneys are drained sequentially by the interlobular, arcuate, and interlobar veins. The lobar veins join to form the main renal vein.

The main renal vein usually lies anterior to the renal artery at the renal hilum. The left renal vein has an average length of 6–10 cm and normally courses anteriorly between the superior mesenteric artery and aorta before emptying into the medial aspect of the IVC. The right renal vein has an average length of 2–4 cm and joins the lateral aspect of the IVC. The longer course of the left renal vein makes the left kidney the preferred choice for donation. The left renal vein receives several tributaries from the left adrenal vein superiorly, the left gonadal vein inferiorly, and the lumbar veins posteriorly before joining the IVC. The right gonadal vein drains into the right renal vein in approximately 8% of cases (8). It is important to identify the prominent venous tributaries preoperatively in patients who will be undergoing renal donation surgery, as these vessels may not be detectable intraoperatively (9). Supernumerary renal veins are more common on the right side. The most common congenital anomaly of the left renal venous system is a circumaortic renal vein, which is seen in up to 17% of patients. A completely retroaortic renal vein is seen in 3% of patients (1). Although renal vein variants are not considered a contraindication to surgery, they should be reported and described when found in patients who are being assessed as possible renal donors (6). A circumaortic renal vein also has management implications for IVC filter placement, because the filter should be placed inferior to the lowest limb of the vein. Plexiform left renal vein refers to a rare variant in which the renal vein divides beyond the renal hilum to form a vascular network and then reunites into a single vein before draining into the IVC (10).

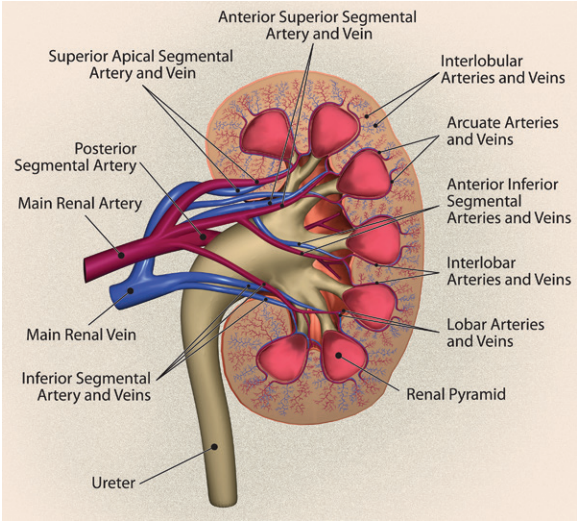

Figure 2. Drawing illustrates the normal arterial and venous supply of the kidney. The main renal artery branches into five segmental arteries, which supply end arteries to the renal parenchyma. The lobar arteries branch into interlobar arteries and then into arcuate arteries, which mark the corticomedullary junction. Venous drainage follows the arterial supply of blood to the kidneys.

Imaging Protocols

Ultrasonography (US) facilitates the acquisition of real-time qualitative and quantitative information regarding the renal vasculature. Computed tomographic (CT) angiography and magnetic resonance (MR) angiography enable the acquisition of purely anatomic information; however, Doppler US has the advantage that it yields physiologic data as well. A native-kidney Doppler US examination should include measurements of the angle-corrected peak systolic velocity (PSV) in the abdominal aorta and renal artery at the origin, middle portion, and hilum; spectral waveforms of the main renal artery and segmental arteries; acceleration times; and acceleration indexes. The PSV in the main renal artery ranges from 60 to 100 cm/sec (11). Acceleration time is the time from the start of systole to peak systole. A normal acceleration time for the main renal artery is less than 70 msec. Acceleration index is the slope of the systolic upstroke, which should be more than 300 cm/sec^2. RAS results in an increased PSV within the stenotic segment of the vessel and an increased acceleration time in the vessel distal to the stenotic segment. The resistive index is calculated by dividing the difference between the PSV and end-diastolic velocity by the PSV and is calculated at the level of the arcuate arteries, with a normal value of 0.60–0.70 (12). The resistive index can be elevated owing to a number of entities, including ureteric obstruc-

tion and intrinsic renal disease (12). Results of spectral analysis of the renal vein may indicate a respiratory fluctuation of flow, with an increase in flow velocity during inspiration. The left renal vein typically exhibits pulsatile variation due to a brief compression of the vein between the aorta and superior mesenteric artery during systole. Although Doppler US offers many advantages, it is technically challenging to perform owing to the depth and small caliber of the renal vasculature. Anatomic variants, large body habitus, and bowel gas can add to the technical difficulty of this examination.

CT is a powerful imaging modality for evaluating the renal vasculature. It offers the advantages of fast image acquisition, excellent spatial resolution, and numerous postprocessing capabilities such as maximum intensity projections and curved planar reformations. Maximum intensity projection images are useful for gaining an overview of the renal vasculature, and curved planar reformation images are useful for inspecting long segments of the vasculature, particularly those of tortuous vessels. CT angiography is the ideal examination for detecting and characterizing renal arterial abnormalities. It is performed by using a rapid contrast material injection rate (5 mL/sec), a scanning delay optimized for arterial enhancement, and thin-section isotropic acquisition that enables optimal postprocessing. However, venous structures are better assessed on delayed phase contrast material–enhanced CT images obtained after an 85-second scanning delay.

In certain patients, MR imaging has unique advantages, as compared with CT and US. In patients with renal dysfunction, in whom iodinated contrast material administration is contraindicated, time-of-flight and steady-state free-precession MR imaging sequences render valuable information. In patients who are able to receive gadolinium-based contrast material, MR angiography with subtraction imaging is an effective way of highlighting the vascular structures. MR angiography is performed with coronal three-dimensional fast low-angle shot (FLASH) imaging by using a test bolus to optimize contrast timing. Multiphasic contrast-enhanced acquisitions also yield additional information regarding the venous structures without the additional radiation exposure required for CT. Endovascular renal stents are better evaluated with CT angiography owing to the blooming artifact seen on MR images.

Processes Affecting the Renal Arteries

Renal Artery Stenosis

RAS is the most common cause of secondary hypertension and is found in 1%–5% of all patients who have hypertension (13). In greater than two-thirds of cases of RAS, focal narrowing of the renal artery lumen is caused by atherosclerosis. The majority of affected individuals are male and older than 50 years. Atherosclerotic renovascular disease correlates with overall atherosclerotic burden, and the prevalence of this condition is higher among patients with known coronary artery disease (14). RAS leads to reduced perfusion to the kidney, which then results in systemic hypertension due to activation of the renin-angiotensin system (14). RAS is also an important factor of end-stage renal disease, particularly in persons older than 50 years (9). RAS caused by atherosclerosis typically occurs at the origin of the renal artery or within the proximal 2 cm of the renal artery (9). When stenosis is detected, careful inspection of the contralateral renal artery is important, as bilateral lesions occur in 30% of cases.

US diagnostic criteria for RAS can be divided into direct signs, which are seen at the site of stenosis, and indirect signs, which are distal to the stenosis (Fig 3) (13). Direct signs include a PSV greater than 200 cm/sec; a renal artery PSV–to–prerenal abdominal aorta PSV ratio higher than 3.5:1.0; the lack of a Doppler US signal, indicating occlusion; and the presence of color artifacts such as aliasing related to turbulence (Table). The flow velocity increases in proportion to the degree of luminal narrowing. Disorderly flow detected at the site of the luminal narrowing manifests as turbulence and/or spectral broadening.

Indirect signs of RAS—that is, those distal to the site of stenosis—include a spectral waveform with a delayed and blunted systolic upstroke known as pulsus parvus et tardus; this finding correlates with an acceleration index lower than 300 cm/sec^2, an acceleration time longer than 70 msec, and a loss of early systolic peak (13). The presence of a pulsus parvus et tardus waveform has a specificity of 96% and a positive predictive value of 92% for the diagnosis of RAS; however, it has a sensitivity of only 43% (11).

CT angiography is the ideal imaging examination for the diagnosis of RAS, with greater than 90% accuracy (Fig 4). Atherosclerotic lesions can have variable amounts of calcification and be concentric or eccentric (9). In addition to directly visualized luminal narrowing, secondary CT signs of hemodynamically significant stenosis include poststenotic dilatation, renal atrophy, and decreased cortical enhancement (9). Although MR angiography has lower spatial resolution compared with CT angiography, it remains useful for the detection of RAS, with reported sensitivities of 90%–100% (15). The advantage of both CT angiography and MR angiography over US is that they facilitate

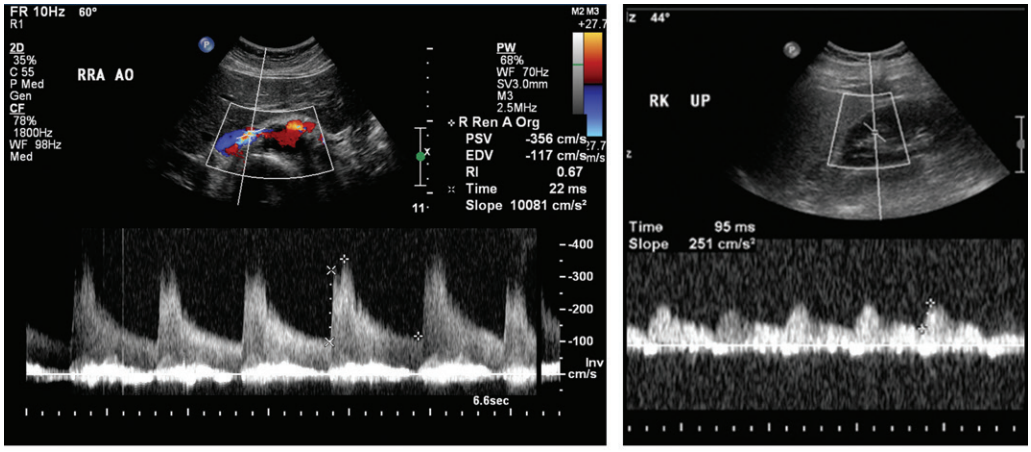

a. **b.**

Figure 3. Direct and indirect US findings in a patient with secondary hypertension due to RAS. **(a)** Transverse US image of the proximal right renal artery *(RRA),* with spectral Doppler imaging at the level of the stenosis, shows an elevated PSV (>200 cm/sec) and aliasing, which indicates turbulent blood flow. *AO* = aorta. **(b)**. Sagittal US image shows a pulsus parvus et tardus waveform distal to the site of stenosis, where there is blunting of the systolic peak with a delayed upstroke. This waveform is quantified on the basis of an acceleration time longer than 70 msec and an acceleration index lower than 300 cm/sec^2. *RK UP* = right kidney upper pole.

US Signs of RAS

Direct US signs
Renal artery PSV > 200 cm/sec
Renal artery PSV–to–prerenal abdominal aorta PSV ratio > 3.5:1.0
Lack of Doppler US signal in cases of occlusion
Doppler US artifacts caused by turbulence (aliasing)
Indirect US signs
Pulsus parvus et tardus (blunted and delayed systolic upstroke)
Acceleration index < 300 cm/sec^2
Acceleration time (ie, time to peak systole) > 70 msec

Note.—Direct US signs are those at the site of vessel narrowing. Indirect US signs are those distal to the site of narrowing.

improved detection and evaluation of accessory renal arteries, which may harbor stenoses and cause secondary hypertension.

Guidelines established by the American College of Cardiology and American Heart Association call for the use of both medication and revascularization strategies to treat patients with RAS (15). Endoluminal stent placement is generally considered superior to balloon angioplasty for addressing atherosclerotic causes of RAS, with higher reported outcome success rates and lower restenosis rates compared with those associated with angioplasty alone (15). Unilateral, nonostial, isolated, short-segment atherosclerotic stenoses are highly suitable for catheter-based interventions. A renal resistive index higher than 0.80 has been suggested as an indicator of poor therapeutic response to revascularization treatment (16). Surgical reconstruction is generally reserved for patients in whom catheter-based treatment of RAS was unsuccessful.

Fibromuscular Dysplasia

Fibromuscular dysplasia (FMD) is a nonatherosclerotic noninflammatory vascular disease of medium-sized and large arteries that results in focal areas of irregular wall thickening (16). FMD is the second most common cause of RAS and is found in younger patients, with a female-to-male ratio of 9:1 (2). The most commonly affected vessel is the renal artery (in 75% of cases) followed by the internal carotid artery (17). FMD results in stenosis, aneurysm, dissection, and occlusion of the involved vessels. FMD is subclassified into three categories based on the involved arterial layer: medial fibroplasia, which accounts for 80%–90% of cases; intimal fibroplasia, which accounts for 10% of cases; and adventitial fibroplasia, which has an unknown frequency.

In contradistinction to atherosclerotic stenoses, which are seen in the proximal renal artery,

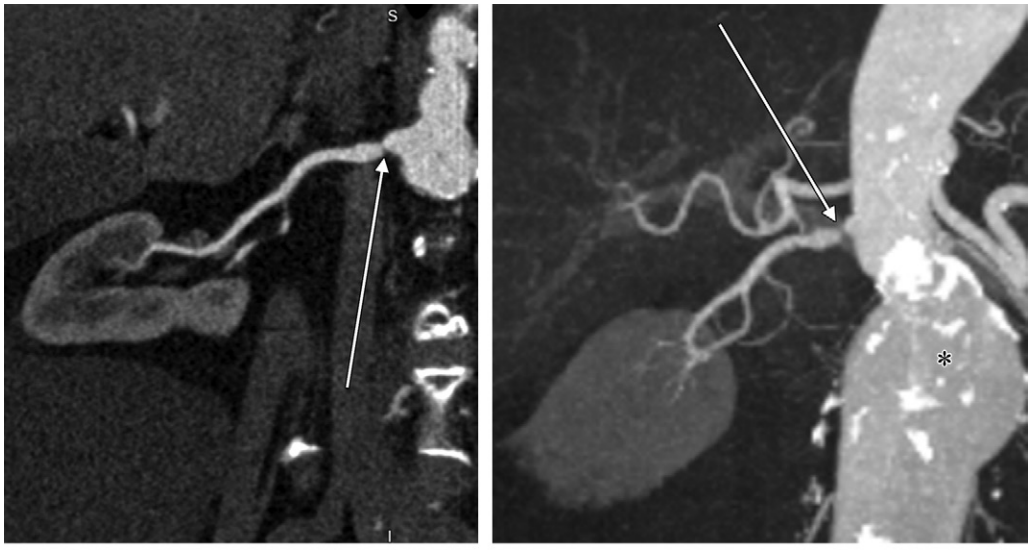

a. b.

Figure 4. Atherosclerotic RAS in an 82-year-old man with refractory hypertension. Coronal curved planar reformatted **(a)** and coronal maximum intensity projection **(b)** images from a CT angiogram show a focal severe short segment of narrowing (arrow) of the proximal renal artery. Additional atherosclerotic changes and a fusiform aneurysm are present in the infrarenal abdominal aorta (* in **b**). Atherosclerotic renovascular disease correlates with overall atherosclerotic burden.

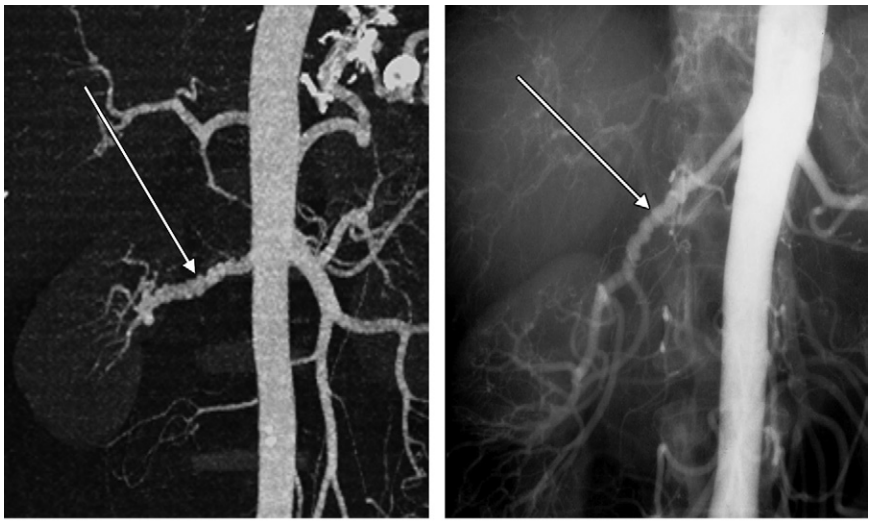

a. b.

Figure 5. FMD in a 52-year-old woman with secondary hypertension. **(a)** Coronal maximum intensity projection CT angiogram shows a "string of pearls" appearance (arrow) of the right main renal artery. This appearance is consistent with fibromedial dysplasia, the most common subtype of FMD. **(b)** Digital subtraction angiogram obtained at the time of percutaneous treatment confirms the presence of multiple alternating areas of narrowing and dilatation (arrow) of the right renal artery. Stenosis in cases of FMD responds exceptionally well to angioplasty.

FMD-related stenoses tend to occur in the middle to distal portion of the renal artery (2). When FMD is discovered in a renal artery, close inspection of the contralateral renal artery is prudent, because FMD occurs bilaterally in two-thirds of patients. Up to 10% of all cases of FMD have associated renal artery aneurysms (RAAs) (18). The most common subtype, medial fibroplasia, is characterized by alternating segments of stenosis and dilatation, which create the "string of pearls" appearance (Fig 5) (17). The intimal fibroplasia subtype is characterized by focal long-segment tubular areas of luminal stenosis. CT angiography has been shown to be 100% sensitive for the diagnosis of FMD, and MR angiography is reported to have a sensitivity of 97% and a specificity of 93% for this diagnosis (19,20).

Percutaneous angioplasty is the treatment of choice for RAS caused by FMD (15). Endoluminal stent placement and surgical bypass are reserved for cases of treatment failure or complications such as dissection. Catheter-based interventions are more likely to cure secondary hypertension in patients with FMD compared to those with atherosclerotic causes of RAS (14).

Renal Artery Entrapment

Extrinsic compression of the renal artery by the crus of the diaphragm or psoas muscle may occur owing to an anomalous course of the

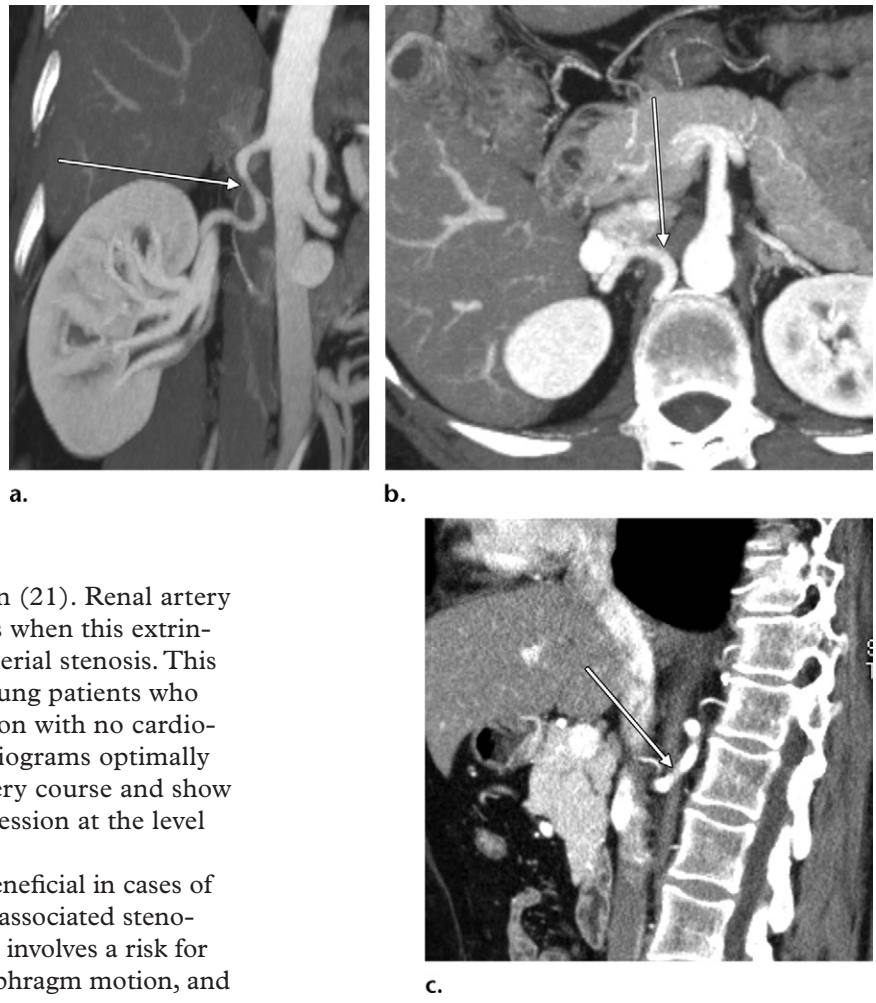

Figure 6. Aberrant course of the right renal artery incidentally detected in a 55-year-old woman. Coronal curved planar reformatted **(a)**, axial maximum intensity projection **(b)**, and sagittal **(c)** images from a CT angiogram show the high origin of the right renal artery (arrow), which courses through the right crus of the diaphragm. This aberrant course predisposes an individual to entrapment and may result in RAS. However, no associated stenosis was detected in this case.

artery—typically a high origin (21). Renal artery entrapment syndrome occurs when this extrinsic compression results in arterial stenosis. This syndrome can manifest in young patients who have renovascular hypertension with no cardiovascular risk factors. CT angiograms optimally depict the aberrant renal artery course and show the extent of extrinsic compression at the level of the diaphragm (Fig 6).

Stent placement may be beneficial in cases of renal artery entrapment with associated stenosis. However, stent placement involves a risk for mechanical failure due to diaphragm motion, and surgical treatment may be necessary.

Renal Artery Dissection

The majority of renal artery dissections are extensions of aortic dissections. Dissections isolated to the renal artery are a known complication of endovascular procedures and blunt abdominal trauma. However, spontaneous renal artery dissection is a rare entity that occurs without a known inciting event. Predisposing factors include FMD, malignancy-related hypertension, severe atherosclerosis, Marfan syndrome, Ehlers-Danlos syndrome, subadventitial angioma, cystic medial necrosis, cocaine abuse, and extreme physical exertion (22). Patients present with nonspecific symptoms, including acute onset of flank pain, decreased renal function, and hypertension.

Spontaneous renal artery dissections most often originate in the distal main renal artery (23). CT angiography is the imaging examination of choice for noninvasive diagnosis of renal artery dissection (Fig 7). CT angiography may show a focal dissection flap, with the true lumen in continuity with the aortic lumen. Often, however, the dissection flap is not visualized on cross-sectional images owing to the small caliber or thrombosis of the renal artery (6). In such cases, only secondary signs of dissection, such as a segment of uniform luminal narrowing, focal vessel cutoff, or distal ischemic changes, may be evident (9,24). Catheter angiography may be used to confirm equivocal cases and plan the endovascular treatment.

Treatment of spontaneous renal artery dissection is based on the stability of the dissection flap and renal function (22). Stable patients are treated conservatively with systemic anticoagulation therapy and observation. For unstable patients, endovascular stent placement has been shown to lead to favorable long-term outcomes and has been suggested as the first-line therapy for revascularization (25).

Renal Artery Aneurysm

Aneurysms of the renal artery are true aneurysms caused by degeneration and weakening of the elastic fibers of the arterial wall, with subsequent expansion caused by high intraluminal pressure. The estimated prevalence of RAAs is approximately 0.1% (23); most of them are detected incidentally in asymptomatic patients (26). However, patients may present with findings of rupture, thrombosis, or embolism. RAAs are associated with systemic

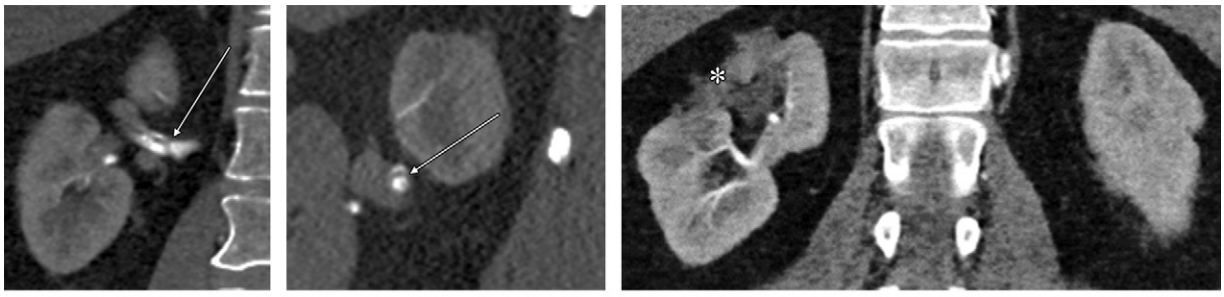

Figure 7. Isolated spontaneous renal artery dissection in a 47-year-old man with acute onset of right flank pain. Coronal (**a**, **c**) and sagittal **(b)** images from a CT angiogram show a dissection flap (arrow in **a** and **b**) in the middle segment of the right renal artery. The aorta (not shown) was free of dissection. **(c)** Ischemic end-organ changes (*) are present in the upper pole of the right kidney. The patient was treated with anticoagulation medication, and the dissection flap was found to be stable at follow-up imaging.

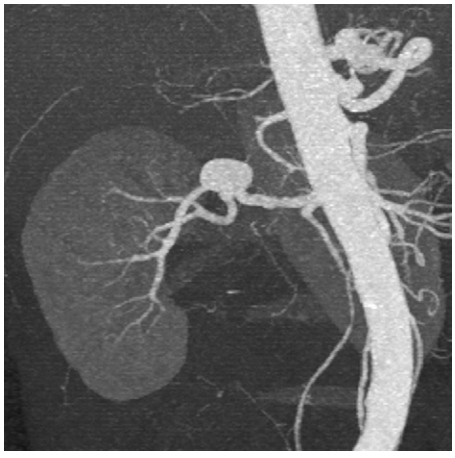

Figure 8. RAA in a 51-year-old woman with hypertension. Maximum intensity projection image from a CT angiogram shows a 2.0-cm saccular aneurysm arising from the branching point of the right renal artery. This is the most common location of RAAs. The subtle undulation of the main renal artery is due to mural irregularity related to underlying atherosclerosis. The patient underwent surgical repair of the aneurysm and was treated with medication for hypertension.

hypertension in 73% of cases. Thirty-four percent of patients have underlying FMD (27).

Most RAAs involve the main renal artery, and the most common site is at the main renal artery bifurcation (60%) (Fig 8) (27). Only 10% of RAAs are intraparenchymal (23). Most RAAs are saccular and noncalcified (28). US images demonstrate an anechoic mass, with the Doppler flow in contiguity with the main renal artery. However, dense aneurysm wall calcification and mural thrombosis may mask the Doppler flow. Nonenhanced CT is useful for assessing the degree of peripheral calcification. It is postulated that mural calcification provides some protection against aneurysm rupture (9). CT angiography is the optimal examination for characterizing RAAs and detecting additional visceral artery aneurysms. Approximately 6.5% of patients with RAAs have aneurysms elsewhere, such as the abdominal aorta and/or splenic artery (27). MR angiography is useful for RAA surveillance, as it does not involve patient exposure to ionizing radiation.

The management of RAAs is based in part on the size of the aneurysm and the clinical setting; however, size does not have a direct correlation with rupture (29). RAAs 1.0–1.5 cm in diameter should be evaluated with surveillance imaging every 1–2 years (30). Patients with RAAs larger than 1.5 cm should be referred for definitive treatment (28). Additional indications for treatment of RAAs include uncontrolled hypertension and symptomatic cases due to peripheral vascular bed embolism. Pregnant women also are at high risk for RAA rupture (28). The mortality rate associated with RAA ruptures is 10% and increases to 50% with pregnancy (23). Patients with branch-type RAAs can be treated with catheter embolization; those with main RAAs can be treated with covered stent placement, surgical ligation, or surgical bypass.

Pseudoaneurysm.—Pseudoaneurysms of the renal artery occur as a result of direct injury to the arterial wall with subsequent disruption and extravasation of the blood contained in the arterial adventitia or surrounding tissues (26). Pseudoaneurysms occur most often in response to iatrogenic or penetrating trauma (31). Multiple intraparenchymal pseudoaneurysms can develop with vasculitis and as a result of amphetamine use (26). A pseudoaneurysm rupture may manifest as hematuria, flank pain, and/or hypotensive shock.

Renal artery pseudoaneurysms typically have a saccular morphology and a direct arterial communication (Fig 9). On gray-scale US images, pseudoaneurysms may mimic renal cysts, and color Doppler US images show the "yin-yang" sign, which represents the turbulent "to-and-fro" flow detected at spectral Doppler US. This

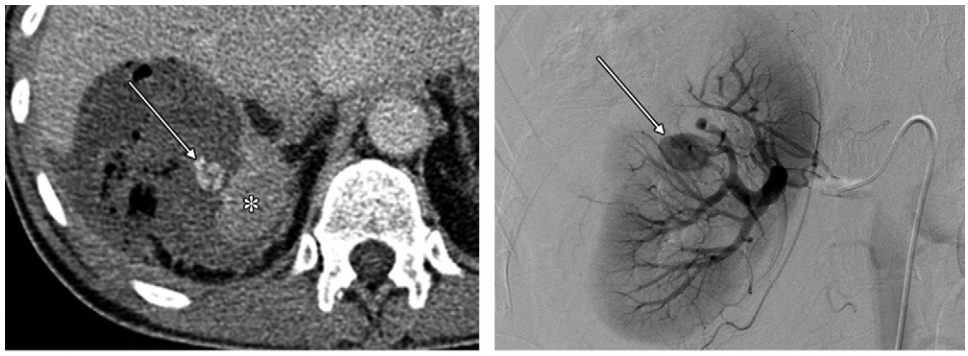

a. b.

Figure 9. Iatrogenic pseudoaneurysm in a 48-year-old woman who had persistent flank pain and hematuria after undergoing robotic partial nephrectomy for papillary renal cell carcinoma in the upper pole of the right kidney. **(a)** Axial CT image shows an intrarenal collection of contrast material (arrow) in the upper pole of the right kidney (*). A heterogeneous collection is present between the upper pole of the right kidney and the liver. Low-attenuating foci represent hemostatic material around the upper pole of the kidney placed at the time of surgery. **(b)** Digital subtraction angiogram obtained at the time of endovascular treatment shows an extravascular pooling of contrast material (arrow), consistent with a pseudoaneurysm, in the upper pole of the kidney. The patient was successfully treated with coil embolization of the distal intrarenal arterial branches, without a decline in renal function.

alternating flow at the pseudoaneurysm neck is due to dynamic pressure gradients that occur between the pseudoaneurysm and the artery from which it arises. CT angiography shows an intrarenal focus of arterial enhancement and offers the advantages of multiplanar reformatting and detection of associated renal injuries. MR imaging is useful for patients with renal impairment, and nonenhanced MR images may show a flow void, which indicates the vascular nature of a lesion.

Small pseudoaneurysms may resolve spontaneously. Patients with pseudoaneurysms larger than 2 cm are at high risk for rupture and require definitive treatment. Treatment with transcatheter embolization in the emergent setting is associated with a success rate of 93% for controlling hemorrhage while preserving the renal parenchyma (32).

Mycotic RAA

Mycotic RAAs result from arterial wall degeneration and disruption that are caused by infectious arteritis. These processes result in pseudoaneurysm formation and a ruptured vessel retained in surrounding inflammatory tissue. Immunosuppression and intravenous drug abuse are known risk factors. Most patients present with signs and symptoms of sepsis (33). Mycotic RAAs can arise from septic emboli from a distant site of infection or, rarely, as a direct complication of pyelonephritis or renal abscess. They have also been associated with renal artery stent placement (26).

As with most pseudoaneurysms, mycotic aneurysms are characterized by a saccular morphology (33). Inflammatory changes are key to determining the diagnosis and may include vessel wall thickening, soft-tissue enhancement, adjacent fat stranding, and/or fluid collections (33). Imaging findings of underlying pyelonephritis or renal abscess also are helpful in suggesting the diagnosis.

Intravenous antibiotic administration is warranted for cases of infected aneurysms. However, aneurysms that are symptomatic or larger than 2 cm may require emergent surgical or endovascular repair (34).

Renal Artery Occlusion

Occlusion of the main renal artery may lead to infarction of the kidney in as little as 60 minutes owing to the lack of collateral blood flow (9). Occlusion may result from thrombosis or thromboembolism. Underlying atherosclerotic disease is often present in cases of acute thrombosis. Embolic disease most often originates from the heart and is due to atrial fibrillation, post–myocardial infarction thrombi, or valvular heart disease (35). However, renal artery embolism is relatively uncommon, occurring in approximately 2% of cases (36). Patients present with an acute onset of flank pain, hematuria, nausea, vomiting, and hypertension; a history of trauma or recent surgery may help determine the diagnosis. Serum lactate dehydrogenase is the most sensitive serologic marker for renal infarction (37). Although renal function is preserved during the acute phase, renal impairment is a known sequela—especially when diagnosis is delayed (38). In cases of acute thrombosis, chronic RAS is protective against renal infarction owing to the development of collateral vessels over time (6).

US can be used to detect areas of renal infarction with complete loss of Doppler signal. However, compared with CT and MR imaging, US has lower sensitivity—especially in the detec-

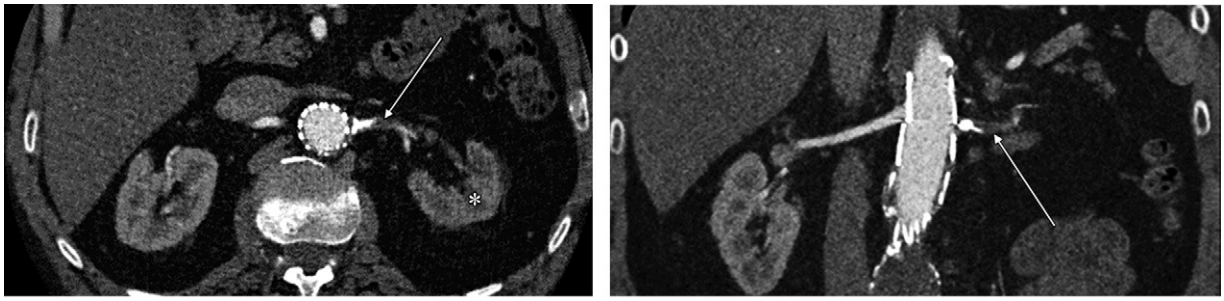

a. b.

Figure 10. Left renal artery thrombosis in a 62-year-old man who had decreased renal function and renovascular hypertension after undergoing abdominal aortic aneurysm repair. Axial **(a)** and coronal **(b)** images from a CT angiogram show a low-attenuating thrombus (arrow) in the proximal left main renal artery and dense atherosclerotic calcification at the left ostium. In **a**, the left kidney is atrophic and has decreased perfusion (*) compared with the perfusion of the right kidney. In cases of acute renal artery occlusion, underlying RAS is protective against renal infarction owing to the development of collateral vessels in the circulation. Only the uncovered portion of the abdominal aortic endograft extends above the renal artery origins to maintain blood flow to the kidneys.

tion of small infarcts. Contrast-enhanced CT images show infarction as a wedge-shaped area of nonenhancement or global nonenhancement of the renal parenchyma. The "cortical rim" sign refers to a 1–3-mm rim of subcortical enhancement caused by the preserved flow of blood supplied from capsular perforating vessels (39). CT is useful for determining the underlying cause, such as dissection, atrial thrombus, or cardiac valve vegetation (Fig 10). CT may also reveal infarcts affecting other organs, such as the spleen; these occur in 34% of patients. Remote infarcts appear as areas of cortical loss and parenchymal retraction. Bilateral renal infarction occurs in 16% of cases, and underlying atrial fibrillation or coagulopathy is the usual cause in such cases (38). Contrast-enhanced MR images show findings similar to those seen at CT. Nonenhanced MR images show variable alterations in renal parenchymal signal intensity, which depend on the age of the infarction. Catheter angiography is the reference-standard imaging examination for detection of renal artery occlusion and is useful for determining the level and degree of occlusion.

Most patients with renal artery occulsion are treated conservatively with hypertension control and anticoagulation therapies, as attempts at revascularization tend to have low success rates (36). Thrombolytic therapy is beneficial only when the renal parenchyma is viable. Patients with global or segmental infarcts who present within 2 days of onset may benefit from endovascular revascularization (36).

Systemic Disorders Affecting the Renal Arteries

Polyarteritis Nodosa

Polyarteritis nodosa is a systemic necrotizing vasculitis that affects medium-sized and small arteries (40). The renal vasculature is the most common site of involvement; it is the involved site in 90% of patients with polyarteritis nodosa (40,41). The nonspecific systemic clinical symptoms of persistent fever, weight loss, and polyarthragia can lead to a delayed diagnosis.

CT images show diffuse enlargement and hypoattenuation of the kidneys (42). T2-weighted MR images show diffuse high signal intensity (42). Multiple small bilateral infarcts of various ages distributed among the interlobar and arcuate arteries also should raise suspicion of underlying vasculitis. Infarcts of other organs, most commonly the spleen, also point to the systemic nature of polyarteritis nodosa. Gastrointestinal tract involvement, as evidenced by bowel wall thickening, is the second most commonly encountered end-organ abnormality (43). Angiography shows multiple microaneurysms of the distal interlobar and arcuate arteries. These microaneurysms are typically 2–3 mm in diameter, which may be beyond the spatial resolution that is possible with CT angiography and MR angiography. However, CT angiography and MR angiography offer the advantage that they show parenchymal changes that are not evident on standard angiograms. The abnormality most commonly detected at CT angiography is RAA; however, stenosis, occlusion, and arterial wall irregularity also may be present (43). The rupture of microaneurysms may result in the spontaneous development of a perinephric hematoma (Fig 11) (41).

Polyarteritis nodosa is usually fatal if it is left untreated; associated renal failure and cardiac and cerebral infarctions are major causes of patient mortality. However, the early initiation of immunosuppressant treatment improves the prognosis (42).

Other Vasculitides

Systemic lupus erythematosus and vasculitis caused by the use of narcotic drugs such as

methamphetamines and cocaine and chemotherapeutic drugs such as vinblastine, cisplatin, and bleomycin can cause findings similar to those of polyarteritis nodosa (44). Neurofibromatosis, Takayasu arteritis, and radiation-induced arteriopathy are rare causes of RAS and RAAs (9).

Neurofibromatosis

Neurofibromatosis type 1 (NF-1) is an autosomal dominant disorder that affects multiple organ systems, including the central nervous system, and predisposes the affected individual to a variety of neoplasms. Vascular disease is the second most common cause of death, after malignancy, in patients with NF-1 (45). It causes a vasculopathy that is postulated to be due to cellular proliferation, degeneration, and eventual fibrosis (45). Although pheochromocytoma is the most common cause of secondary hypertension in adult patients with NF-1, the secondary hypertension in pediatric patients with this disorder is most often caused by RAS (46). Vascular abnormalities are found in 0.4%–6.4% of patients with NF-1, and the renal artery is the most commonly involved artery, being affected in 41% of patients with associated vascular abnormalities (45). Unlike atherosclerotic stenosis, NF-1–associated stenoses often occur in patients younger than 50 years, spare the renal artery origin, are long and tapered, and extend into segmental and intrarenal branches (45). The stenoses involved with NF-1 are bilateral in 32% of patients. Less commonly, NF-1 manifests with RAAs. Compared with atherosclerotic RAAs, the aneurysms associated with NF-1 are often intrarenal (45). Surgical treatment of NF-1–related RAS is preferred over endovascular therapy because of the high rate of restenosis associated with angioplasty (45).

Takayasu Arteritis

Takayasu arteritis is an idiopathic inflammatory vascular disorder most commonly found in young women of Asian descent (47). Takayasu arteritis typically affects large and medium-sized elastic arteries and manifests with stenoses, occlusions, and less commonly aneurysms (48). Although the great arch vessels are the most commonly involved, renal artery involvement also is common. CT angiography and MR angiography show smooth luminal stenoses and complete occlusions. An additional benefit of CT angiography and MR angiography, as compared with catheter angiography, is the depiction of vessel wall thickening. In fact, vessel wall thickening, edema, and enhancement are early inflammatory changes that precede stenosis (49). Vessel wall changes, even in the absence of luminal changes, are reliable parameters for monitoring disease activity in patients being treated with immunosuppressive therapy (49). Revascularization with catheter-based techniques is prone to restenosis owing to the ongoing inflammatory nature of Takayasu arteritis. Surgical bypass may be required for cases of long-standing renal artery lesions and has been shown to improve hypertension and renal function (48).

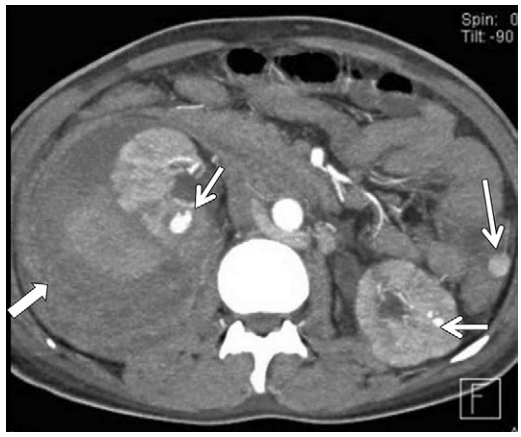

Figure 11. Polyarteritis nodosa in a 26-year-old man who presented with hematuria. Axial CT image shows multiple small aneurysms (short thin arrows) in the kidneys and spleen (long thin arrow) and a large right perinephric hematoma (thick arrow). (Reprinted, with permission, from reference 43.)

Arteriovenous Communications

Arteriovenous Malformation.—Renal arteriovenous malformations (AVMs) are developmental anomalies in which an abnormal connection is present between a renal artery and renal vein owing to a nidus consisting of a network of abnormal vessels (29). Renal AVMs are usually symptomatic; gross hematuria results from the rupture of small venules into calyces that is caused by abnormally increased intravascular pressure (29). Other symptoms include renovascular hypertension, high-output cardiac failure, and flank pain.

Renal AVMs are classified into cavernous and cirsoid types. Cavernous AVMs are supplied by a single arterial feeding vessel. Cirsoid AVMs are supplied by multiple arterial feeding vessels that have a corkscrew appearance (29). Doppler US images demonstrate turbulent high flow in the vascular channels, with low resistance waveforms (Fig 12). CT angiography with multiformat reconstruction is useful for delineating the feeding artery, nidus, and early draining vein. CT is also valuable for searching for complications of renal AVMs, such as subcapsular or perinephric hematoma (41). MR imaging is useful for patients with renal impairment, because even on nonenhanced images, prominent flow voids can be appreciated within the lesion (44).

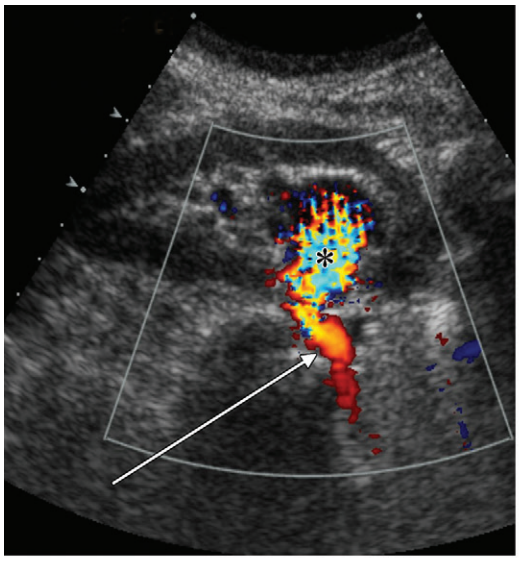

a.

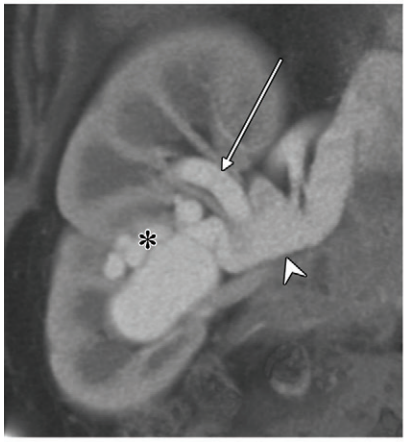

b.

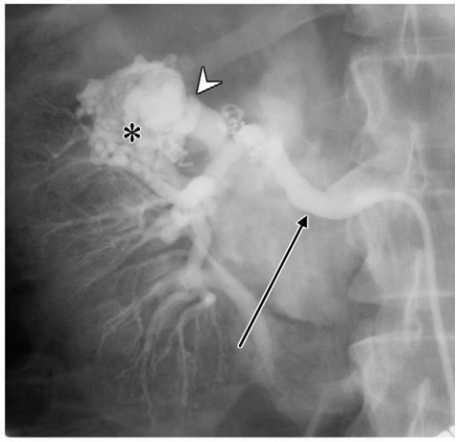

c.

Figure 12. AVM in a patient with hematuria. **(a)** Sagittal color Doppler US image of the right kidney shows a feeding artery (arrow) leading to a nidus of vessels with turbulence. The turbulence manifests as aliasing (*), which is indicative of high blood flow. **(b)** Coronal reformatted CT angiogram better delineates the feeding artery (arrow), nidus (*), and dilated draining vein (arrowhead). **(c)** Angiogram obtained at the time of endovascular treatment confirms the presence of the AVM (*) and depicts the dilated early draining vein (arrowhead). The arrow points to the feeding artery.

Endovascular treatment involving alcohol ablation of the nidus and feeding vessels is the treatment of choice (29). For larger AVMs, coil embolization may be required; however, care must be taken to avoid losing coils in the venous circulation (29).

Arteriovenous Fistula.—An arteriovenous fistula (AVF) is an abnormal direct connection of an artery to a vein without an intervening capillary bed (41). Most renal AVFs are acquired, and they usually have an iatrogenic cause such as percutaneous nephrostomy or result from penetrating trauma. In up to 18% of cases, AVFs occur after renal biopsy. Idiopathic cases are postulated to occur when an RAA ruptures into an adjacent vein. Most patients are asymptomatic, although they may present with hematuria and flank pain.

Spectral Doppler US images of AVFs show increased flow velocity, decreased arterial resistance, and arterial waveforms in the outflow vein. The resistive index of the feeding artery may be dramatically decreased—to between 0.30 and 0.40 (50). At CT angiography and MR angiography, renal AVFs are characterized by a single dilated feeding artery and early enhancement of a dilated draining vein (Fig 13) (41). Renal parenchyma overlying the fistula may become atrophic secondary to ischemia that is caused by vascular shunting.

Most renal AVFs resolve spontaneously without treatment. Transcatheter embolization is the treatment of choice for symptomatic cases; compared with surgical treatment, it facilitates greater preservation of renal function. Although a variety of endovascular embolic strategies have been described, coil embolization is the most commonly used (32). Surgical treatment may be required for larger renal AVFs.

Arteriovenous Connections Associated with Renal Cell Carcinoma.—Both AVFs and AVMs may be associated with renal malignancy. Renal AVMs are postulated to result from angiogenic factors that are caused by the malignancy and induce the formation of abnormal vascular connections (29). AVFs associated with renal malignancies are

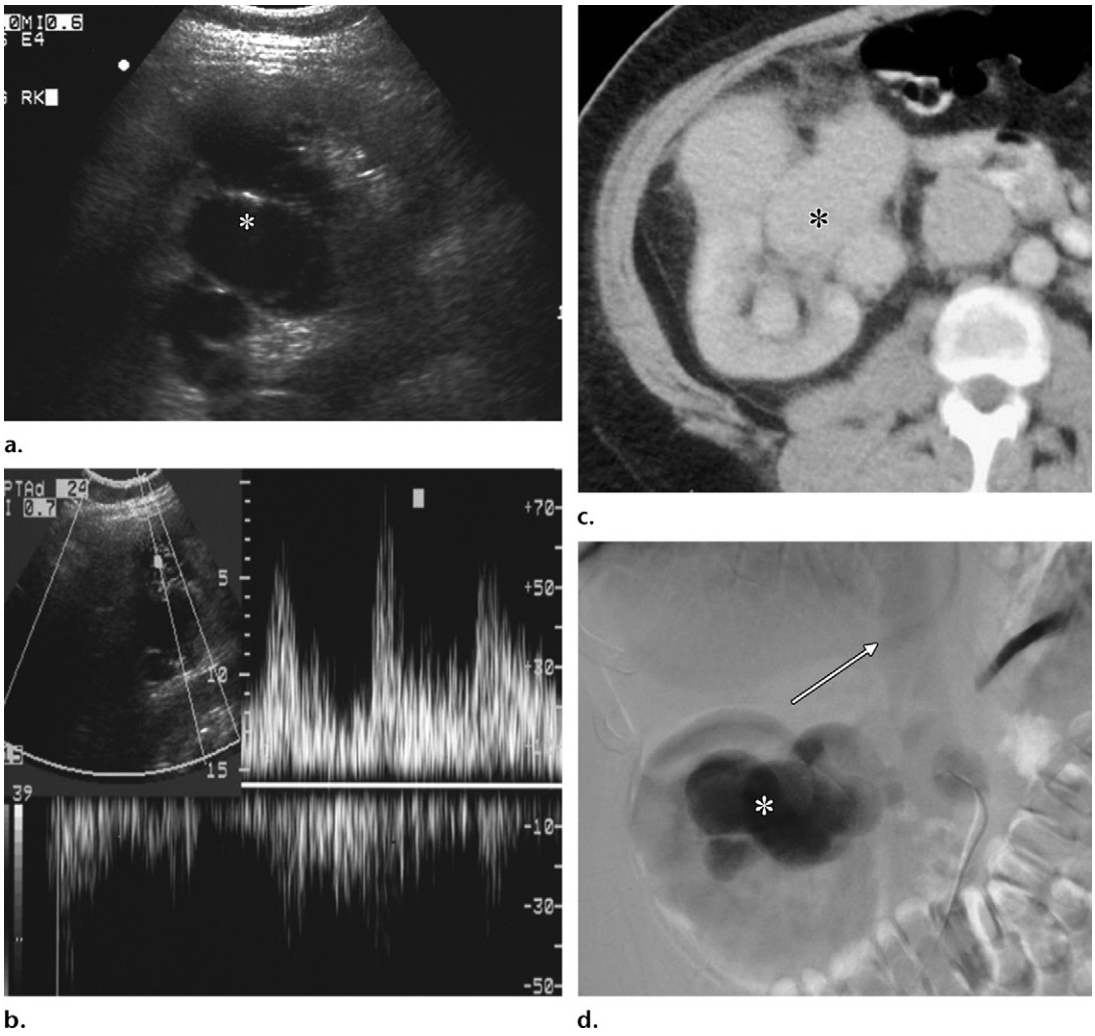

Figure 13. Large AVF. **(a)** Transverse gray-scale US image shows an anechoic cystlike mass (*) in the right kidney. **(b)** Transverse spectral Doppler US image shows arterial waveforms, which confirm the vascular nature of the mass. **(c)** Axial contrast-enhanced CT image shows dilated vascular channels (*) in the central region of the right kidney. **(d)** Preoperative angiogram shows a dilated feeding artery (*) and an early draining vein, with early opacification of the IVC (arrow).

thought to result from tumor invasion and the development of communicating vascular spaces within necrotic tumors (51). Fistulas in metastatic lesions from renal cell carcinoma also have been reported (51). Patients may present with gross hematuria and hypertension. When the fistula is large, shunting of blood flow may result in high-output cardiac failure. The AVFs seen with renal cell carcinoma usually are small (Fig 14). When the AVF is large, the vascular communication may obscure the underlying renal mass (52). Surgical management of renal cell carcinoma, with resection of the AVF, leads to improved hypertension and heart function in symptomatic patients.

Secondary Ureteropelvic Junction Obstruction Caused by Crossing Vessels

Obstruction of the ureteropelvic junction results from impedance in the normal flow of urine from the renal pelvis into the proximal ureter, which leads to renal collecting system dilatation. A crossing vessel compressing or distorting the ureteropelvic junction may be the primary cause of the ureteropelvic junction obstruction, or it may coexist with other causes (53). A crossing vessel can be seen in 29%–46% of cases of ureteropelvic junction obstruction (44). Accessory vessels supplying the lower pole of the kidney may arise from the renal vessels, aorta, vena cava, or iliac vessels. Patients may present with acute renal colic or chronic back pain, and the symptoms may be related to periods of increased fluid intake. Other signs include hematuria and pyelonephritis.

CT angiography is highly sensitive and specific for defining crossing vessels and is preferred over catheter angiography, which may not depict crossing veins (Fig 15). Most often, the crossing vessel is anterior to the ureteropelvic junction, although it may be posterior to this junction in 5%–10% of cases (44). Diuretic-phase techne-

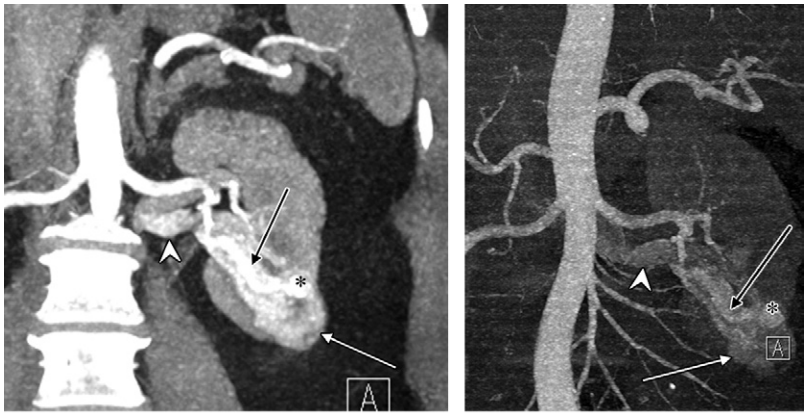

a. b.

Figure 14. AVF associated with renal cell carcinoma of the lower pole of the kidney in a 56-year-old woman. Coronal thin **(a)** and thick **(b)** maximum intensity projection images show an enhancing mass (white arrow) in the lower pole of the left kidney. The prominent vascular communication (*) in the superior margin of the mass was created by a prominent feeding artery (black arrow) and early draining vein (arrowhead).

tium Tc 99m mertiatide (MAG_3) or technetium Tc 99m pentetic acid (DTPA) renal scintigraphy is useful for assessing the functional importance of the renal collecting system dilatation.

Surgery is indicated for impaired renal function or worsening symptoms. Previously, the standard surgical intervention was open pyeloplasty. However, the recent advent of minimally invasive endourologic techniques—namely, endopyelotomy—and laparoscopic or robot-assisted laparoscopic pyeloplasty has led to improvements in postoperative recovery, although these procedures may be more technically challenging (9). It is especially important to recognize and consider the presence of crossing vessels owing to the associated risk for hemorrhage during minimally invasive therapies. Furthermore, the presence of crossing vessels decreases the success rate with antegrade endopyelotomy—reportedly from 86% to 42% (54). In addition, intraoperative preservation of crossing vessels is important for preserving renal function, as these vessels are end arteries, which lack an anastomotic communication. Thus, the preoperative detection of crossing vessels at the ureteropelvic junction, whether these are the primary cause of obstruction or an incidental finding, can have important implications for surgical planning.

Processes Affecting the Renal Veins

Nutcracker Syndrome

The nutcracker phenomenon occurs when the left renal vein is compressed between the aorta and superior mesenteric artery and consequently results in left renal vein hypertension. The term *nutcracker syndrome* refers to the clinical signs and symptoms that can result from this anatomic finding (55). Nutcracker syndrome has also been reported in association with a retroaortic course of the left renal vein, which results in a compression between the aorta and vertebral body (56). Nutcracker syndrome is commonly found in thin young females. A history of recent substantial weight loss also is implicated in cases of nutcracker syndrome (57). Hematuria and flank pain are common clinical symptoms (58). Additional symptoms related to pelvic congestion syndrome also may be present. Compression of the left renal vein can cause left renal vein–to–gonadal vein reflux that results in lower limb varices and varicoceles in males (56).

The normal angle between the superior mesenteric artery and abdominal aorta is greater than 45° (59). In abnormal cases, the superior mesenteric artery branches from the aorta at an acute angle of 35° or less, with steep caudal descent, and compresses the left renal vein (56,59). Doppler US has been suggested as the initial imaging examination of choice for the diagnosis of nutcracker syndrome; it has a reported sensitivity and specificity of 78% and 100%, respectively (60). With US, venous stenosis can be detected by comparing the peak velocity in the vein proximal to the aortic transition with the peak velocity in the vein distal to the aortic transition and comparing the anteroposterior diameter of the left renal vein at the level of the renal hilum with this diameter at the point of the superior mesenteric artery crossing. A reduction in the inner diameter of the left renal vein between the renal hilum and point of stenosis by a factor of at least 3 in a supine patient and by a factor of at least 5 in a standing patient for at least 15 minutes is a criterion for US-based diagnosis of nutcracker syndrome (59). CT facilitates better anatomic delineation of the superior mesenteric artery, aorta, and left renal vein. The "beak" sign refers to the abrupt narrowing, with a triangular configuration, at the aortomesenteric portion of the left renal vein depicted at CT (Fig 16). This finding is reported to have a sensitivity of 91.7% and a specificity of 88.9% (58). Sagittal CT angiography and MR angiography are useful for

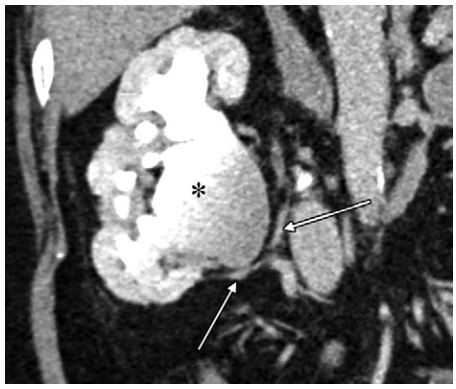

Figure 15. Ureteropelvic junction obstruction in a 59-year-old woman with hematuria. Coronal CT urogram shows right hydronephrosis and a dilated renal pelvis (*). A crossing vessel (arrows) is present at the ureteropelvic junction. The crossing vessel is a small accessory renal vein of the lower pole of the kidney draining into the right gonadal vein. The patient underwent successful robot-assisted laparoscopic pyeloplasty with intraoperative identification of the crossing vessel.

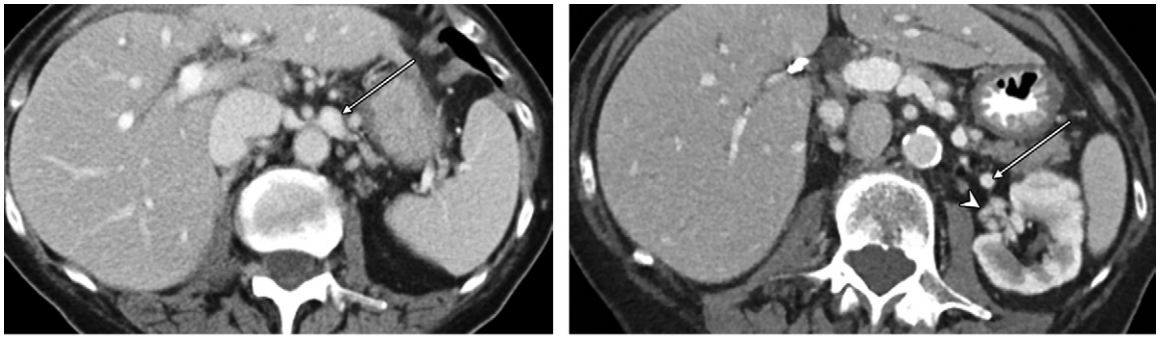

a. **b.**

Figure 16. Nutcracker syndrome in an 86-year-old woman with recent weight loss. **(a)** Axial CT image through the left renal vein shows the beak sign (arrow)—that is, an abrupt luminal narrowing and triangular configuration of this vessel as it crosses between the aorta and superior mesenteric artery. **(b)** Axial CT image inferior to the renal vein shows multiple perirenal collateral vessels (arrowhead) and opacification of the left gonadal vein (arrow).

assessing the angle between the proximal superior mesenteric artery and aorta. When present, prominent collateral draining vessels—including the paralumbar, gonadal, and hemiazygos veins—suggest marked obstruction of blood flow. Angiography can be used in conjunction with pressure gradient measurements to confirm the diagnosis in equivocal cases. A pressure gradient of greater than 2 mm Hg between the IVC and renal vein suggests outflow obstruction (57).

Surgical and endovascular treatments are available for symptomatic cases of nutcracker syndrome (56). Open surgical procedures include renal vein transposition, superior mesenteric artery transposition, renal autotransplantation, and gonadocaval bypass. Endovascular stent placement in the renal vein has a high success rate; however, its long-term efficacy is unknown.

Renal Vein Thrombosis

Thrombosis that leads to narrowing or occlusion of the renal vein can be caused by a bland or tumor thrombus. Patients present with gross hematuria, flank pain, and signs of renal failure. Risk factors of bland renal vein thrombosis include glomerulonephritis, collagen vascular disease, diabetes, and trauma.

Renal vein thrombosis occurs more commonly on the left side—probably because of the longer course of the left renal vein. Rarely, left renal vein thrombosis is due to extension of a thrombus from the left gonadal vein. US is usually the initial examination performed in cases of clinically suspected renal vein thrombosis. US images may show a loss of corticomedullary differentiation in addition to renal enlargement. Color Doppler US images show absent flow in the renal vein and reversal of diastolic flow in the main renal artery. On CT images, acute renal vein thrombosis is seen as a hypoattenuating filling defect within a dilated renal vein (Fig 17) (2). Secondary signs include delayed renal cortical enhancement, edema in the renal sinus and perinephric space, and ipsilateral renal enlargement. In chronic cases of renal vein thrombosis, multiple collateral vessels may develop. The sensitivity and specificity of contrast-enhanced MR venography for diagnosis of renal vein thrombosis have been shown to be similar to those of CT (61). Trauma-induced renal vein thrombosis almost invariably manifests with additional renal artery or parenchymal injury (Fig 18) (62,63).

Anticoagulant therapy is the treatment of choice for bland renal vein thrombosis. Thrombolytic therapy can be administered in cases of

a.

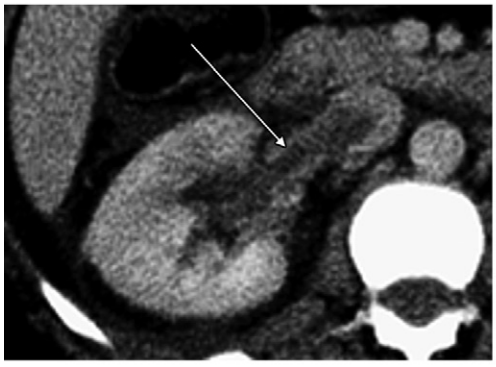

b.

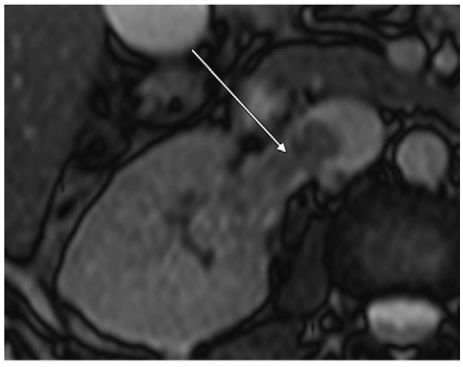

c.

Figure 17. Right renal vein thrombosis in a 29-year-old woman with acute-onset right flank pain. **(a)** Coronal CT image shows an enlarged edematous right kidney (*). **(b)** Axial CT image through the right kidney shows an intraluminal filling defect (arrow) in the right renal vein, extending into the IVC. **(c)** The defect (arrow) can also be detected on an axial nonenhanced steady-state free precession MR image. The patient was treated with systemic anticoagulation therapy, and follow-up imaging findings indicated resolution of the thrombosis.

a.

b.

Figure 18. Renal vein thrombosis in a 14-year-old boy with a history of blunt trauma and severe renal laceration. Axial **(a)** and coronal **(b)** contrast-enhanced CT images show a low-attenuating filling defect (arrows) within the segmental right renal veins, extending into the main renal vein and IVC. There are extensive posttraumatic changes in the right kidney, including a perinephric hematoma and grade 5 laceration, as defined by the American Association for the Surgery of Trauma as a laceration that results in a completely shattered kidney. This patient was not a candidate for anticoagulation therapy owing to the renal trauma, which was managed nonsurgically. A jugular approach was used to place a retrievable suprarenal IVC filter for temporary protection from pulmonary embolus.

bilateral renal vein thrombosis with acute renal failure. Placement of a suprarenal vena cava filter may be considered for select patients with thrombosis extending into the IVC.

Renal Vein Tumor Thrombosis

Renal Cell Carcinoma.—The malignancy that most commonly invades the renal veins is renal cell carcinoma. Patients may present with gross hematuria, flank pain, and a flank mass. Secondary symptoms include lower extremity edema, right-sided varicocele that does not collapse with recumbency, and dilated superficial abdominal veins.

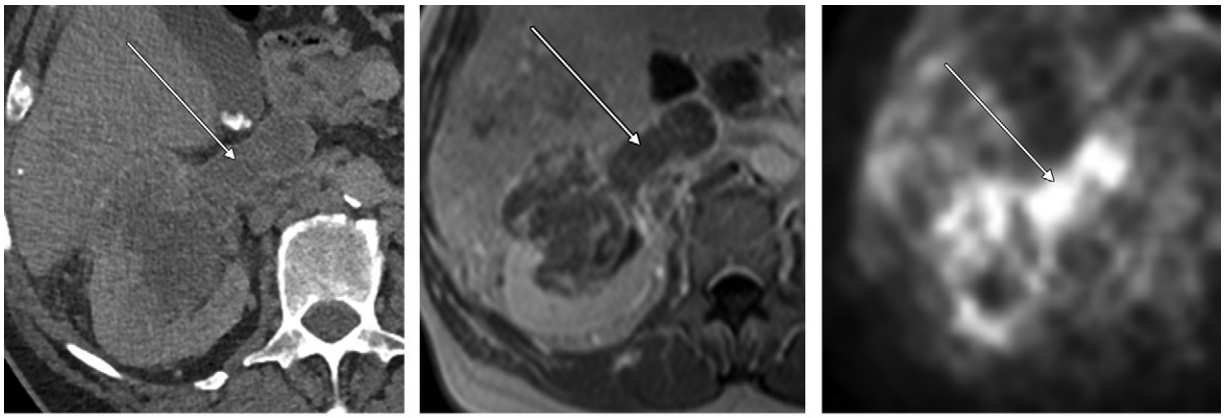

a. b. c.

Figure 19. Tumor thrombus secondary to renal cell carcinoma in a 65-year-old man. **(a)** Axial CT image shows a mass in the right kidney, with an intraluminal filling defect in the right renal vein extending into the IVC (arrow). **(b)** The filling defect (arrow) is also demonstrated on an axial contrast-enhanced T1-weighted in-phase MR image. **(c)** Axial fluorine 18 fluorodeoxyglucose positron emission tomographic image shows activity that corresponds to the filling defect seen in **a** and **b** and confirms the presence of a metabolically active tumor thrombus (arrow). The patient underwent open radical nephrectomy with IVC thrombectomy.

Determining the extent of renal vein involvement is crucial for surgical planning. Although enhancement within the thrombus is indicative of malignant involvement, lack of enhancement does not exclude the presence of a tumor thrombus. Compared with CT and MR imaging, US has lower sensitivity for detection of tumor thrombi (64). CT has been shown to enable an accurate determination of the extent of a tumor thrombus in cases of renal cell carcinoma (Fig 19). However, MR imaging remains the examination of choice for this application because it can depict a coexistent bland thrombus. Loss of the normal flow void within the renal vein is a useful finding for detecting renal vein thrombosis at nonenhanced MR imaging. The superior extent of a thrombus is important for surgical planning, and imaging should be performed within 7–10 days of surgery, as these tumors may propagate rapidly.

Nephrectomy with tumor thrombectomy is the standard treatment for patients with renal vein involvement by renal cell carcinoma. Long-term cancer-free survival is achieved after surgical resection in up to 40%–65% of patients. Anticoagulation therapy is needed if a bland thrombus is present in addition to a tumor thrombus.

Other Tumors.—Aside from renal cell carcinoma, many other tumors can invade a renal vein. Adrenocortical carcinoma is an uncommon tumor that rarely has been shown to invade the renal veins and IVC. Complete resection is the only curative treatment for patients with adrenocortical carcinoma. Tumor extension into the renal veins and IVC is not a contraindication to surgery (Fig 20).

Wilms tumor is the most common renal and abdominal malignancy of childhood. Intravascular extension of a Wilms tumor occurs in 6% of individuals (Fig 21). There is no substantial difference in survival outcomes between persons with and those without intravascular extension. However, intravascular extension is associated with an increased incidence of surgical complications.

Figure 20. Adrenocortical carcinoma with intravascular extension in a 74-year-old man. Coronal CT image shows a large right adrenal gland mass (*) extending into the expanded IVC (arrow) and left renal vein (arrowhead).

Upper tract urothelial cell carcinoma has been reported to extend into the renal veins; however, this is an unusual finding (65). Renal angiomyolipomas, while histologically benign, can extend into the renal veins and IVC—albeit rarely—and result in a pulmonary embolism (66). Rarely, renal oncocytoma demonstrates intravascular extension that mimics that of renal cell carcinoma (67). However, intravascular extension of oncocytoma does not portend a poor prognosis.

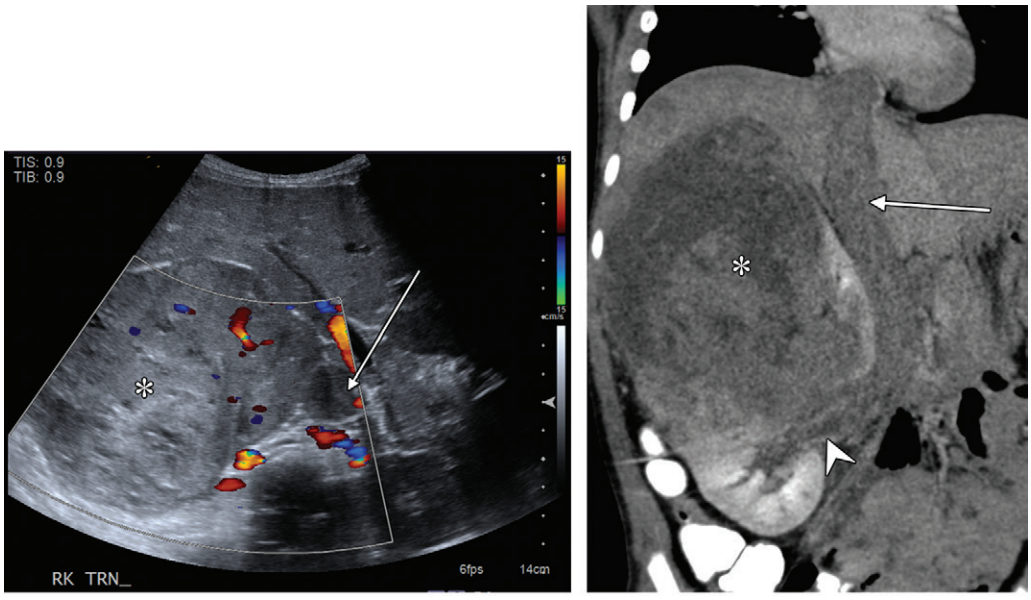

a. b.

Figure 21. Wilms tumor with intravascular extension in a 3-year-old girl with abdominal pain and distention. **(a)** Transverse color US image of the right kidney shows a large heterogeneous mass (*) in the right kidney. A tumor thrombus (arrow) is expanding the IVC. **(b)** Coronal CT image shows a heterogeneous mass (*) in the upper pole of the right kidney, with a tumor thrombus (arrowhead) in the right renal vein and extending into the IVC (arrow).

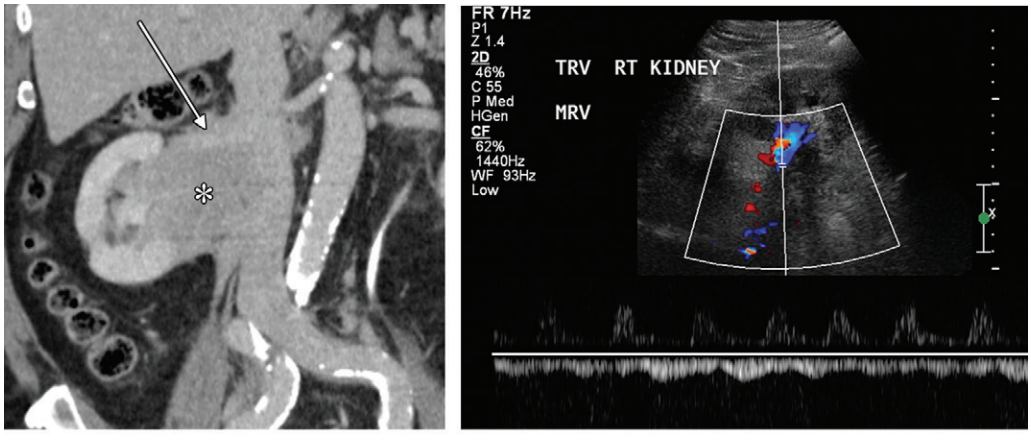

a. b.

Figure 22. Renal lymphoma encasing the renal vasculature in an 83-year-old man. **(a)** Coronal CT image shows an infiltrative mass (*) in the right renal sinus. The mass partially encases the right renal vein (arrow) and right renal artery (not shown). **(b)** Findings on a transverse *(TRV)* color US image confirm that the right renal vein is patent despite substantial tumor encasement. *MRV* = main renal vein.

Rarely, lymphoma may invade the renal vein although venous encasement is more commonly encountered (68). However, occlusion of renal vasculature by lymphoma is rare despite extensive tumor encasement because of the pliable nature of the tumor (Fig 22).

Renal Vein Leiomyosarcoma

Leiomyosarcoma is a primary malignant tumor arising from smooth muscle. Approximately 5% of leiomyosarcomas arise from large blood vessels, with the IVC being the most common site. Renal vein leiomyosarcoma occurs more commonly in female individuals and manifests as abdominal pain, weight loss, and rarely, pulmonary embolism (69).

Renal vein leiomyosarcoma arises more commonly on the left side—probably because of the longer course of the left renal vein. The tumor expands the renal vein and may extend into the renal parenchyma and IVC (Fig 23). CT and MR images show homogeneous contrast enhancement of the tumor; however, solely peripheral enhancement may be present. Occasionally,

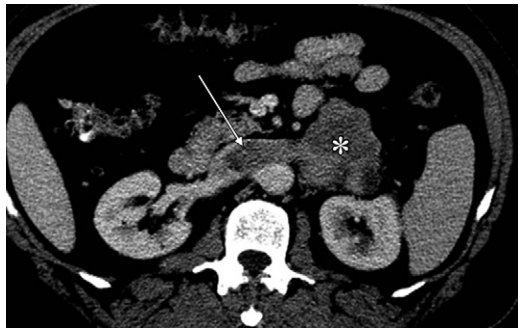

Figure 23. Primary leiomyosarcoma of the left renal vein in a 59-year-old man who presented with low back pain. Axial CT image shows a heterogeneous mass (*) expanding the left renal vein, with intravascular extension into the IVC (arrow). The kidney itself is not involved. The patient underwent en bloc surgical resection with left nephrectomy and adrenalectomy, as well as IVC thrombectomy.

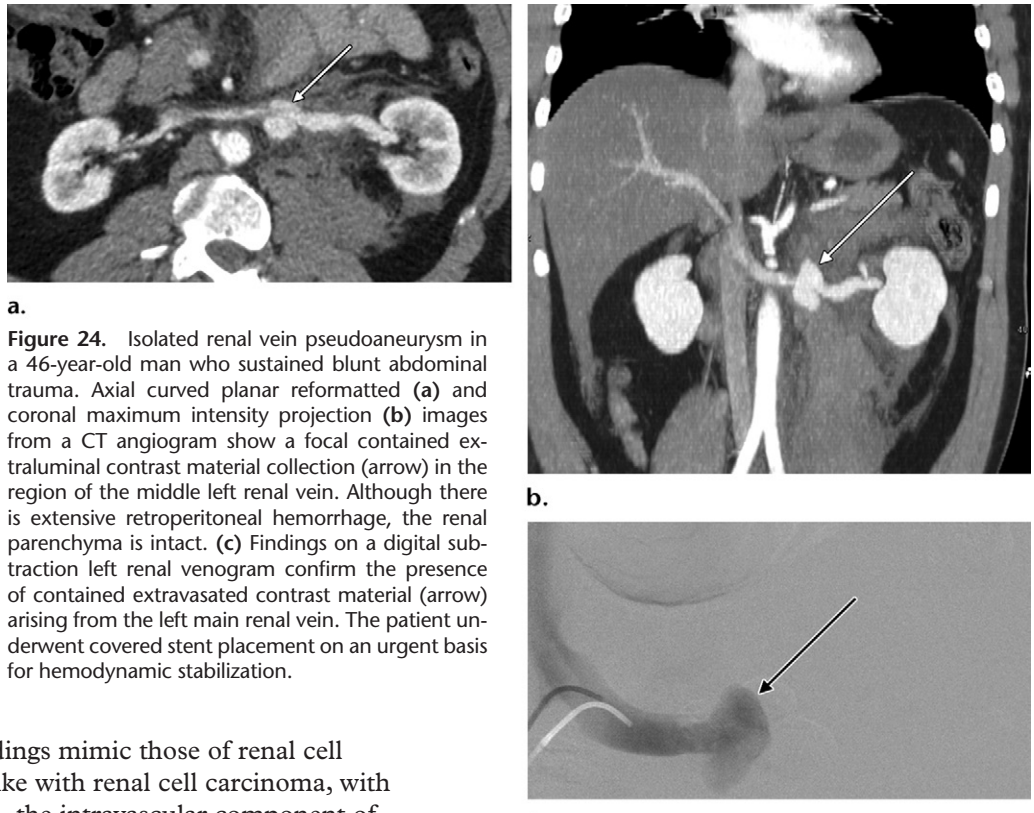

a.

b.

c.

Figure 24. Isolated renal vein pseudoaneurysm in a 46-year-old man who sustained blunt abdominal trauma. Axial curved planar reformatted **(a)** and coronal maximum intensity projection **(b)** images from a CT angiogram show a focal contained extraluminal contrast material collection (arrow) in the region of the middle left renal vein. Although there is extensive retroperitoneal hemorrhage, the renal parenchyma is intact. **(c)** Findings on a digital subtraction left renal venogram confirm the presence of contained extravasated contrast material (arrow) arising from the left main renal vein. The patient underwent covered stent placement on an urgent basis for hemodynamic stabilization.

the imaging findings mimic those of renal cell carcinoma. Unlike with renal cell carcinoma, with leiomyosarcoma, the intravascular component of the tumor is larger than the intrarenal component (70). The diagnosis of renal vein leiomyosarcoma should be suspected when a mass with intravascular extension into the renal vein is present without an associated solid organ mass.

The treatment for patients with leiomyosarcoma is en bloc surgical resection. Neoadjuvant chemotherapy and radiation therapy may have an important role before surgery (70).

Renal Vein Trauma

Injury to the renal vein is a rare complication of abdominal trauma; it is seen in 1%–3% of trauma cases (71). Injury to the central renal veins can result in substantial morbidity and mortality, with an associated risk for subsequent renal impairment in surviving patients. These injuries are typically accompanied by additional signs of abdominal trauma, and affected patients usually are symptomatic at presentation. A contained central renal vein rupture that creates a venous pseudoaneurysm can be readily detected with CT angiography. The finding of a direct defect in the renal vein wall, with extravasated contrast material in continuity with the vessel lumen, enables confident diagnosis. Additional renovascular and parenchymal abnormalities are expected associated findings; isolated renal vein pseudoaneurysms are rare (Fig 24). Retroperitoneal hemorrhage surrounding the renal vein also is a helpful sign of underlying vascular injury. Endovascular treatment of the renal vein pseudoaneurysm with covered stent placement has been shown to be effective for hemodynamic stabilization and preserving renal function (71).

Conclusion

Imaging is critical for the diagnosis and management of renovascular pathologic conditions, and as

such, the radiologist has a crucial role. In addition, many of these entities are difficult to recognize solely with clinical evaluation, and imaging may be the only means of diagnosis. Therefore, interrogation of the renal arteries and veins should be an essential part of the search protocol at cross-sectional imaging of the abdomen. Recognition of the vascular nature of these entities will help direct patient care and help to avoid unnecessary additional workup and potentially dangerous biopsy. In addition, an understanding of the imaging protocols used to address renovascular pathologic conditions will help radiologists be highly effective when describing findings to consulting clinicians.

References

1. Standring S, Gray HA. Gray's anatomy: the anatomical basis of clinical practice. 40th ed. Edinburgh, Scotland: Churchill Livingstone, 2008.
2. Urban BA, Ratner LE, Fishman EK. Three-dimensional volume-rendered CT angiography of the renal arteries and veins: normal anatomy, variants, and clinical applications. RadioGraphics 2001;21(2):373–386, questionnaire 549–555.
3. Natsis K, Piagkou M, Skotsimara A, Protogerou V, Tsitouridis I, Skandalakis P. Horseshoe kidney: a review of anatomy and pathology. Surg Radiol Anat 2014;36(6):517–526.
4. Glodny B, Petersen J, Hofmann KJ, et al. Kidney fusion anomalies revisited: clinical and radiological analysis of 209 cases of crossed fused ectopia and horseshoe kidney. BJU Int 2009;103(2):224–235.
5. Flors L, Leiva-Salinas C, Ahmad EA, et al. MD CT angiography and MR angiography of nonatherosclerotic renal artery disease. Cardiovasc Intervent Radiol 2011;34(6):1151–1164.
6. Falesch LA, Foley WD. Computed tomograpy angiography of the renal circulation. Radiol Clin North Am 2016;54(1):71–86.
7. Dyer RB, Regan JD, Kavanagh PV, Khatod EG, Chen MY, Zagoria RJ. Percutaneous nephrostomy with extensions of the technique: step by step. RadioGraphics 2002;22(3):503–525.
8. Barber B, Horton A, Patel U. Anatomy of the origin of the gonadal veins on CT. J Vasc Interv Radiol 2012;23(2):211–215.
9. Liu PS, Platt JF. CT angiography of the renal circulation. Radiol Clin North Am 2010;48(2):347–365, viii–ix.
10. Gupta A, Gupta R, Singal R. Congenital variations of renal veins: embryological background and clinical implications. J Clin Diagn Res 2011;5(6):1140–1143.
11. Pellerito JS, Polak JF. Introduction to vascular ultrasonography. 6th ed. Philadelphia, Pa: Saunders/Elsevier, 2012.
12. Tublin ME, Bude RO, Platt JF. Review. The resistive index in renal Doppler sonography: where do we stand? AJR Am J Roentgenol 2003;180(4):885–892.
13. Granata A, Fiorini F, Andrulli S, et al. Doppler ultrasound and renal artery stenosis: an overview. J Ultrasound 2009;12(4):133–143.
14. Creager MA, Loscalzo J, Dzau VJ. Vascular medicine: a companion to Braunwald's heart disease. Philadelphia, Pa: Elsevier Saunders, 2006.
15. Hirsch AT, Haskal ZJ, Hertzer NR, et al. ACC/AHA 2005 Practice Guidelines for the management of patients with peripheral arterial disease (lower extremity, renal, mesenteric, and abdominal aortic): a collaborative report from the American Association for Vascular Surgery/Society for Vascular Surgery, Society for Cardiovascular Angiography and Interventions, Society for Vascular Medicine and Biology, Society of Interventional Radiology, and the ACC/AHA Task Force on Practice Guidelines (Writing Committee to Develop Guidelines for the Management of Patients With Peripheral Arterial Disease)—endorsed by the American Association of Cardiovascular and Pulmonary Rehabilitation; National Heart, Lung, and Blood Institute; Society for Vascular Nursing; TransAtlantic Inter-Society Consensus; and Vascular Disease Foundation. Circulation 2006;113(11):e463–e654.
16. Radermacher J, Chavan A, Bleck J, et al. Use of Doppler ultrasonography to predict the outcome of therapy for renal-artery stenosis. N Engl J Med 2001;344(6):410–417.
17. Olin JW, Sealove BA. Diagnosis, management, and future developments of fibromuscular dysplasia. J Vasc Surg 2011;53(3):826–836.e1.
18. Neymark E, LaBerge JM, Hirose R, et al. Arteriographic detection of renovascular disease in potential renal donors: incidence and effect on donor surgery. Radiology 2000;214(3):755–760.
19. Beregi JP, Louvegny S, Gautier C, et al. Fibromuscular dysplasia of the renal arteries: comparison of helical CT angiography and arteriography. AJR Am J Roentgenol 1999;172(1):27–34.
20. Willoteaux S, Faivre-Pierret M, Moranne O, et al. Fibromuscular dysplasia of the main renal arteries: comparison of contrast-enhanced MR angiography with digital subtraction angiography. Radiology 2006;241(3):922–929.
21. Singham S, Murugasu P, Macintosh J, Murugasu P, Deshpande A. Left main renal artery entrapment by diaphragmatic crura: spiral CT angiography. Biomed Imaging Interv J 2010;6(2):e11.
22. Kanofsky JA, Lepor H. Spontaneous renal artery dissection. Rev Urol 2007;9(3):156–160.
23. Moore WS, ed. Vascular and endovascular surgery: a comprehensive review. 7th ed. Philadelphia, Pa: Elsevier Saunders, 2006.
24. Lacombe M. Isolated spontaneous dissection of the renal artery. J Vasc Surg 2001;33(2):385–391.
25. Pellerin O, Garçon P, Beyssen B, et al. Spontaneous renal artery dissection: long-term outcomes after endovascular stent placement. J Vasc Interv Radiol 2009;20(8):1024–1030.
26. Cura M, Elmerhi F, Bugnogne A, Palacios R, Suri R, Dalsaso T. Renal aneurysms and pseudoaneurysms. Clin Imaging 2011;35(1):29–41.
27. Henke PK, Cardneau JD, Welling TH 3rd, et al. Renal artery aneurysms: a 35-year clinical experience with 252 aneurysms in 168 patients. Ann Surg 2001;234(4):454–462; discussion 462–463.
28. Nosher JL, Chung J, Brevetti LS, Graham AM, Siegel RL. Visceral and renal artery aneurysms: a pictorial essay on endovascular therapy. RadioGraphics 2006;26(6):1687–1704; quiz 1687 .
29. Chimpiri AR, Natarajan B. Renal vascular lesions: diagnosis and endovascular management. Semin Intervent Radiol 2009;26(3):253–261.
30. Khosa F, Krinsky G, Macari M, Yucel EK, Berland LL. Managing incidental findings on abdominal and pelvic CT and MRI. II. White paper of the ACR Incidental Findings Committee II on Vascular Findings. J Am Coll Radiol 2013;10(10):789–794.
31. Jesinger RA, Thoreson AA, Lamba R. Abdominal and pelvic aneurysms and pseudoaneurysms: imaging review with clinical, radiologic, and treatment correlation. RadioGraphics 2013;33(3):E71–E96.
32. Ginat DT, Saad WE, Turba UC. Transcatheter renal artery embolization: clinical applications and techniques. Tech Vasc Interv Radiol 2009;12(4):224–239.
33. Raman SP, Fishman EK. Mycotic aneurysms: a critical diagnosis in the emergency setting. Emerg Radiol 2014;21(2):191–196.
34. Lee WK, Mossop PJ, Little AF, et al. Infected (mycotic) aneurysms: spectrum of imaging appearances and management. RadioGraphics 2008;28(7):1853–1868.
35. Amilineni V, Lackner DF, Morse WS, Srinivas N. Contrast-enhanced CT for acute flank pain caused by acute renal artery occlusion. AJR Am J Roentgenol 2000;174(1):105–106.
36. Lopez VM, Glauser J. A case of renal artery thrombosis with renal infarction. J Emerg Trauma Shock 2010;3(3):302.
37. Lessman RK, Johnson SF, Coburn JW, Kaufman JJ. Renal artery embolism: clinical features and long-term follow-up of 17 cases. Ann Intern Med 1978;89(4):477–482.
38. Antopolsky M, Simanovsky N, Stalnikowicz R, Salameh S, Hiller N. Renal infarction in the ED: 10-year experience and review of the literature. Am J Emerg Med 2012;30(7):1055–1060.
39. Ambesh P, Lal H. Renal cortical rim sign. Abdom Imaging 2015;40(7):2914–2915.

40. Kumar V, ed. Robbins and Cotran's pathologic basis of disease. 8th ed. Philadelphia, Pa: Saunders, 2010.
41. Kawashima A, Sandler CM, Ernst RD, Tamm EP, Goldman SM, Fishman EK. CT evaluation of renovascular disease. RadioGraphics 2000;20(5):1321–1340.
42. Ozaki K, Miyayama S, Ushiogi Y, Matsui O. Renal involvement of polyarteritis nodosa: CT and MR findings. Abdom Imaging 2009;34(2):265–270.
43. Singhal M, Gupta P, Sharma A, Lal A, Rathi M, Khandelwal N. Role of multidetector abdominal CT in the evaluation of abnormalities in polyarteritis nodosa. Clin Radiol 2016;71(3):222–227.
44. Sidhu R, Lockhart ME. Imaging of renovascular disease. Semin Ultrasound CT MR 2009;30(4):271–288.
45. Oderich GS, Sullivan TM, Bower TC, et al. Vascular abnormalities in patients with neurofibromatosis syndrome type I: clinical spectrum, management, and results. J Vasc Surg 2007;46(3):475–484.
46. Han M, Criado E. Renal artery stenosis and aneurysms associated with neurofibromatosis. J Vasc Surg 2005;41(3):539–543.
47. Gotway MB, Araoz PA, Macedo TA, et al. Imaging findings in Takayasu's arteritis. AJR Am J Roentgenol 2005;184(6):1945–1950.
48. Weaver FA, Kumar SR, Yellin AE, et al. Renal revascularization in Takayasu arteritis-induced renal artery stenosis. J Vasc Surg 2004;39(4):749–757.
49. Kissin EY, Merkel PA. Diagnostic imaging in Takayasu arteritis. Curr Opin Rheumatol 2004;16(1):31–37.
50. Hélénon O, Melki P, Correas JM, Boyer JC, Moreau JF. Renovascular disease: Doppler ultrasound. Semin Ultrasound CT MR 1997;18(2):136–146.
51. Rodgers MV, Moss AJ, Hoffman M, Lipchik EO. Arteriovenous fistulae secondary to renal cell carcinoma: clinical and cardiovascular manifestations—report of a case. Circulation 1975;52(2):345–350.
52. Prando A, Prando D, Prando P. Renal cell carcinoma: unusual imaging manifestations. RadioGraphics 2006;26(1):233–244.
53. Grasso M, Caruso RP, Phillips CK. UPJ obstruction in the adult population: are crossing vessels significant? Rev Urol 2001;3(1):42–51.
54. Van Cangh PJ, Nesa S. Endopyelotomy: prognostic factors and patient selection. Urol Clin North Am 1998;25(2):281–288.
55. Kurklinsky AK, Rooke TW. Nutcracker phenomenon and nutcracker syndrome. Mayo Clin Proc 2010;85(6):552–559.
56. Ahmed K, Sampath R, Khan MS. Current trends in the diagnosis and management of renal nutcracker syndrome: a review. Eur J Vasc Endovasc Surg 2006;31(4):410–416.
57. Kaufman JA, Lee MJ. Vascular and interventional radiology: the requisites. St Louis, Mo: Mosby, 2004.
58. Gulleroglu K, Gulleroglu B, Baskin E. Nutcracker syndrome. World J Nephrol 2014;3(4):277–281.
59. Zhang H, Li M, Jin W, San P, Xu P, Pan S. The left renal entrapment syndrome: diagnosis and treatment. Ann Vasc Surg 2007;21(2):198–203.
60. Takebayashi S, Ueki T, Ikeda N, Fujikawa A. Diagnosis of the nutcracker syndrome with color Doppler sonography: correlation with flow patterns on retrograde left renal venography. AJR Am J Roentgenol 1999;172(1):39–43.
61. Zhang LJ, Wu X, Yang GF, et al. Three-dimensional contrast-enhanced magnetic resonance venography for detection of renal vein thrombosis: comparison with multidetector CT venography. Acta Radiol 2013;54(10):1125–1131.
62. Kau E, Patel R, Fiske J, Shah O. Isolated renal vein thrombosis after blunt trauma. Urology 2004;64(4):807–808.
63. Shariat SF, Roehrborn CG, Karakiewicz PI, Dhami G, Stage KH. Evidence-based validation of the predictive value of the American Association for the Surgery of Trauma kidney injury scale. J Trauma 2007;62(4):933–939.
64. Kallman DA, King BF, Hattery RR, et al. Renal vein and inferior vena cava tumor thrombus in renal cell carcinoma: CT, US, MRI and venacavography. J Comput Assist Tomogr 1992;16(2):240–247.
65. Cilliers G, Naidoo A, Ackermann C, Parsons JJ, Andronikou S. Renal vein thrombosis in transitional cell carcinoma. Australas Radiol 2007;51(Spec No):B62–B63.
66. Celik SU, Kocaay AF, Sevim Y, Cetinkaya OA, Atman ED, Alacayir I. Renal angiomyolipoma with caval extension and pulmonary fat embolism: a case report. Medicine (Baltimore) 2015;94(31):e1078.
67. Hes O, Michal M, Síma R, et al. Renal oncocytoma with and without intravascular extension into the branches of renal vein have the same morphological, immunohistochemical and genetic features. Virchows Arch 2008;452(3):285–293.
68. Sheth S, Ali S, Fishman E. Imaging of renal lymphoma: patterns of disease with pathologic correlation. RadioGraphics 2006;26(4):1151–1168.
69. Aguilar IC, Benavente VA, Pow-Sang MR, et al. Leiomyosarcoma of the renal vein: case report and review of the literature. Urol Oncol 2005;23(1):22–26.
70. Maturen KE, Vikram R, Wu AJ, Francis IR. Renal vein leiomyosarcoma: imaging and clinical features of a renal cell carcinoma mimic. Abdom Imaging 2013;38(2):379–387.
71. Monroe EJ, Kogut MJ, Ingraham CR. Traumatic renal vein pseudoaneurysm. J Vasc Surg Cases 2015;1(2):157–160.